LMM-Assisted Breast Cancer Treatment Target Segmentation with Consistency Embedding

Kwanyoung Kim*1, Yujin Oh*2, Sangjoon Park*3,4, Hwa Kyung Byun⁵, Jin Sung Kim†3,6, Yong Bae Kim†3, Jong Chul Ye†1

- ¹ Kim Jae Chul Graduate School of AI, KAIST
- 2 Department of Radiology, Massachusetts General Hospital
- ³ Department of Radiation Oncology, Yonsei, University College of Medicine
 - ⁴ Institute for Innovation in Digital Healthcare, Yonsei University
 - 5 Department of Radiation Oncology, Yongin Severance Hospital 6 Oncosoft Inc.

{cubeyoung}@kaist.ac.kr, {yujin.oh}@havard.edu, {depecher89, hkbuyn05, jinsung, ybkim3}@yuhs.ac, {jong.ye}@kaist.ac.kr

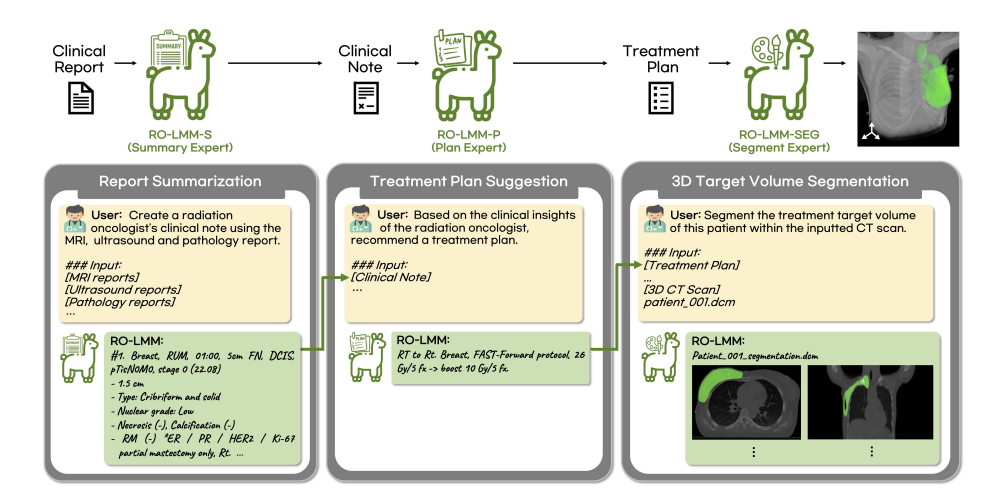


Fig. 1: RO-LMM as an assistant large multimodal model (LMM) in the field of radiation oncology. The model seamlessly covers various tasks such as clinical report summarization, radiation treatment plan suggestion, and plan-guided target volume segmentation. All the patient information and any potential personally identifiable information are de-identified, and the clinical data usage is approved by IRB.

Abstract. Recent advancements in Artificial Intelligence (AI) have profoundly influenced medical fields, by providing tools to reduce clinical workloads. However, most AI models are constrained to execute unimodal tasks, in stark contrast to the comprehensive approaches utilized by medical professionals. To address this, here we present RO-LMM, a multipurpose large multimodal model (LMM) tailored for the field of radiation

^{*} These authors contributed equally to this work

[†] Corresponding authors

oncology. This model covers series of tasks within clinical workflow, adept at clinical report summarization, radiation treatment plan suggestion, and plan-guided target volume segmentation. In particular, to perform consecutive clinical tasks, we further present a novel Consistency Embedding Fine-Tuning (CEFTune) technique, which boosts LMM's robustness to noisy inputs while preserving the capability of handling clean inputs, and transform this concept into LMM-driven segmentation framework as Consistency Embedding Segmentation (CESEG). Experimental results on multi-centre cohorts demonstrate our RO-LMM's promising performance for multiple clinical tasks with generalization capabilities.

1 Introduction

Recently, the emergence of a new generation of AI models, known as foundation models, marks a significant departure from previous paradigms [34]. These foundation models are now capable of achieving state-of-the-art performance (SOTA) in a wide range of domains, including tasks such as multimodal reasoning, image-to-text generation, image captioning, and text-guided image segmentation [3, 10, 12, 25, 27, 31].

These characteristics signify a potential paradigm shift in how AI can be integrated into medical practices, which inherently rely on multimodal information for comprehensive clinical decision-making. Furthermore, this gives an opportunity of overcoming limitations of now over 500 FDA-approved AI models, which are mainly specialized for a specific task with unimodal information [21]. Specifically, in contrast to these unimodal AIs, generalist medical AIs can encompass a holistic understanding of clinical workflows, which can receive and reason a variety of medical data, including imaging modalities, electronic health records, laboratory results, genomics, and even clinical reports [34, 39, 41, 46, 50].

Inspired by this paradigm shift in medical AIs, here we present RO-LMM, a prototype of a multi-purpose medical large multimodal model (LMM), tailored to support the clinical workflow in radiation oncology. RO-LMM is adept at performing a variety of clinical tasks: (1) It efficiently summarizes extensive patient histories and examination results into concise but informative clinical notes. Additionally, it is capable of (2) proposing appropriate treatment plans from a clinical expert perspective and (3) delineating radiation target volumes on 3-dimensional (3D) computed tomography (CT) scans consistent with the proposed treatment plans. This multifaceted functionality demonstrates a significant alignment with the expertise of clinical professionals. To the best of our knowledge, our prototype for assisting in the radiation oncology workflow is the first work. As for an initial trial, we opted for a phased approach, starting with high prevalence cancer types requiring relatively standardized radiotherapy based solely on CT imaging, i.e., breast cancer.

In the course of the aforementioned sequential tasks, the inevitable accumulation of errors in generations arises on both treatment plan suggestion and target volume segmentation task. To address this issue, we firstly explore Noisy Embedding Fine-Tuning (NEFTune) [19] which involves injecting uniform noise

into embeddings during the training for our targeted tasks. To further enhance the model's applicability, we introduce a novel consistency regularization method, bolstered by our pioneering Consistency Embedding Fine-Tuning (CEFTune) technique, which add regularization loss to enforce the consistency between the prediction given noisy and clean inputs. Expanding beyond text-related tasks, we apply these concepts to 3D segmentation tasks, resulting in Noisy Embedding Segmentation (NESEG) and Consistency Embedding Segmentation (CESEG). These advancements collectively contribute to a marked improvement in the model's generalization capabilities in both internal and external validation. Our contributions can be summarized as:

- We propose a comprehensive framework, denoted as RO-LMM, wherein LMM assists the entire workflow of radiation oncology for breast cancer treatment.
- We explore noise augmentation and consistency, and propose a novel training approach, such as CEFTune, NESEG, and CESEG.
- Through experiments on both internal and external datasets on real clinical breast cancer data, we demonstrated that RO-LMM outperforms baseline methods.

2 Related Works

2.1 Instruction Fine-tuning

Instruction fine-tuning has been emerged as a pivotal technique for augmenting model responsiveness in the field of natural language processing (NLP). The simplicity and effectiveness of this approach have been introduced in numerous works, with a notable scale-up facilitated by advancements of large language models (LLMs) such like GPT-3 [2], ChatGPT [36], and GPT-4 [37]. Notably, a pioneering contribution, Self-Instruct [47], involves fine-tuning of foundation models using instruction-output pairs generated from InstructGPT [38]. This methodology, along with similar approaches, has led to diverse language model variants, including Alpaca [42], Vicuna [4], Dolly [8], and a series of LLaMA [43,44], by exhibiting promising performance across a wide range of tasks. In the medical domain, Chat-Doctor [52], Med-Alpaca [14], PMC-LLaMA [49], and Asclepius [24] have been fine-tuned for clinical question-answering (QA) task. Although these models demonstrate robust performance for diverse QA benchmarks, there is a notable gap in their applicability for the practical clinical workflow in a specific domain, such as radiation oncology, which serves as our targeted focus.

2.2 Stabilizing LLM Fine-tuning with Noise

To enhance the robustness of language models against noisy input, various strategies have been explored. Approaches such as SMART [20], FreeLB [54], and R3F [1] employ adversarial training methods, introducing small Gaussian perturbations in embedding dimensions to optimize the model's performance against noise. Aparting from the adversarial training, LSNR [17] takes a different

4 Kim. K Y et al.

approach by directly optimizing the smoothness of each layer of the language model. More recently, NEFTune [19] improves LLM performance during fine-tuning by simply adding random noise into the embedding vectors during training. In the context of this study, we extend NEFTune by incorporating the concept of consistency regularization. This extension aims to further improve the robustness and generalization capabilities of language models when faced with noisy input.

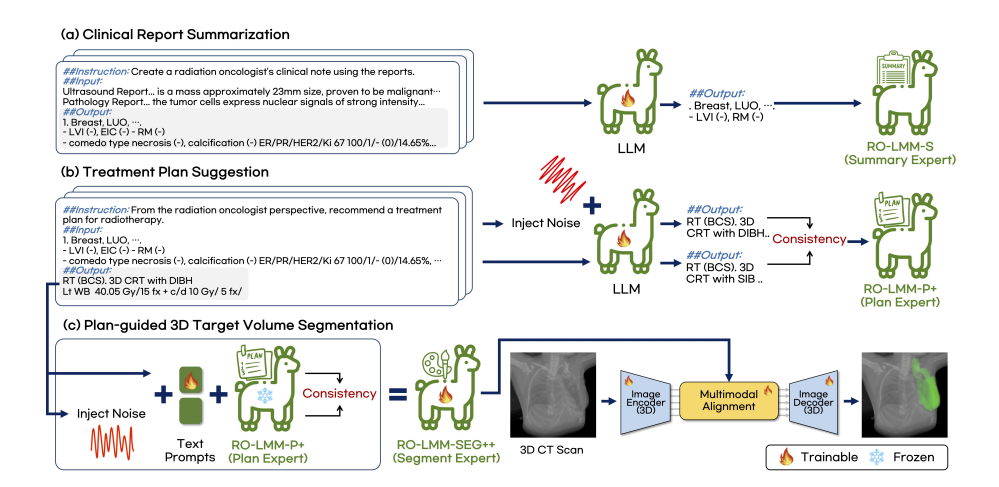


Fig. 2: Training schematics of the multi-purpose RO-LMM for three different tasks. (a) RO-LMM-S for clinical note summarization. (b) RO-LMM-P++ for radiation treatment plan suggestion. (c) RO-LMM-SEG++ for plan-guided target volume segmentation.

2.3 Language-driven Image Segmentation

Recent research in the field of image segmentation has been emerged to incorporate linguistic ability, such like language-driven semantic segmentation [26], open-vocabulary segmentation [11,29,51], referring segmentation [48], and reasoning segmentation [25]. Language-driven segmentation has triggered a paradigm shift in medical domain, where multimodal knowledge is inevitable. For instance, LViT [28] and ConTEXTualNet [18] introduce text-driven chest X-ray radiography segmentation.

Target volume segmentation in the field of radiation oncology is more challenging, due to its intrinsic need for considerations of the clinical aspects beyond the image, such as overall cancer stage, treatment aim, pathological findings, and so on [5,6,15]. Recent research on clinical context-aware breast cancer radiotherapy delineation has demonstrated that the multimodal AI outperforms the traditional unimodal AI by a substantial margin, particularly when labeled datasets are scarce [35]. Unlike previous approaches, we incorporate treatment plans generated by LMM directly from clinical reports, which aligns seamlessly with actual clinical workflows in radiation oncology.

3 Methods

In this section, we provide a detailed methodology for our proposed approach, which is designed for sequential text generation tasks, including summarization and suggestions, as well as text-driven image segmentation, as illustrated in Figure 2. In Sec 3.1, we describe text-related fine-tuning approaches that yield report summarization and plan suggestion, respectively. In Sec 3.2, we introduce a novel segmentation approach that involves injecting noise and regularizing consistency to the text embedding for improving robustness of plan-guided 3D target volume segmentation.

3.1 Consistency Embedding Fine-tuning for Clinical LMM

To realize the multi-purpose LMM with expertise in clinical report summarization and radiation treatment plan suggestion, we conduct instruction fine-tuning for LLaMA2 [44]. Considering the intended objective of each task, we adopt separate strategies to acquire task-specific expertise, namely RO-LMM-S (summary expert) and RO-LMM-P (plan expert). We train a summary expert using collected notes. During inference, the summary expert receives raw clinical reports, just like in the training scenario. However, for the plan expert, there is a discrepancy between the training and inference scenarios. In other words, we opt to use the training set made up of collected notes instead of generated notes, mainly due to cost concerns and the inherent nature of our framework, which generates output sequentially as illustrated in Figure 1. In contrast to training, our model takes the generated notes as input for inference. To enhance robustness for the noisy input, Noisy Embedding Fine-Tuning (NEFTune) [19] which inject uniform noise into embedding is also an effective naive solution to handle noisy inputs in this task. However, a crucial consideration arises from the nature of the generated notes, which may lie closer to clean inputs (collected notes) or deviate towards noisy inputs. To address this, it is essential to train the model to handle both clean and noisy inputs. To preserve the robustness facilitated by NEFTune while enforcing consistency between the prediction given clean and noisy inputs, we introduce Consistency Embedding Fine-Tuning (CEFTune), resulting in RO-LMM-P+ $+^{\dagger}$. More details are as follows.

Revisiting Noise Embedding Fine-Tuning. NEFTune has been recently introduced to enhance the performance of instruction fine-tuning. This approach involves injecting a random noise vector into embeddings during the training process as follows:

$$\mathcal{L}_{\text{NEFTune}}(\theta) = \mathbb{E}_{(\mathbf{x}_{\text{txt}}^{\text{emb}}, \mathbf{y}_{\text{txt}}) \sim D} \mathcal{L}_{\text{ce}}(f_{\theta}(\tilde{\mathbf{x}}_{\text{txt}}^{\text{emb}}), \mathbf{y}_{\text{txt}}),$$

$$\tilde{\mathbf{x}}_{\text{txt}}^{\text{emb}} = \mathbf{x}_{\text{txt}}^{\text{emb}} + (\alpha/\sqrt{LC})\boldsymbol{\epsilon}, \quad \boldsymbol{\epsilon} \sim \mathcal{U}(-1, 1)$$
(1)

where $\mathbf{x}_{\mathrm{txt}}^{\mathrm{emb}} \in \mathbb{R}^{B \times L \times C}$ is the embedding of data, B denotes batch size, L is token length, C is embedding dimension, $\tilde{\mathbf{x}}_{\mathrm{txt}}^{\mathrm{emb}}$ is perturbed embedding, $f_{\theta}(\cdot)$ represents

^{† &#}x27;+', '++' denotes the adoption of NEFTune, and CEFTune, respectively

the model parameterized by θ , \mathbf{y}_{txt} is the label of text sample. They demonstrated that the effectiveness of incorporating a random noise vector adjusted based on token length, which yields robust results in most fine-tuning scenarios.

Consistency Embedding Fine-Tuning. To bolster the model's capability in handling both noisy and clean inputs for treatment plan suggestion task, we incorporate a regularization loss to encourage consistency as follows:

$$\mathcal{L}_{\text{CEFTune}}(\theta) = \mathcal{L}_{\text{NEFTune}}(\theta) + \lambda \mathcal{R}(\theta, \theta^{-}),$$
where $\mathcal{R}(\theta, \theta^{-}) = d(\mathcal{T}(f_{\theta}(\tilde{\mathbf{x}}_{\text{txt}}^{\text{emb}})), \mathcal{T}(f_{\theta^{-}}(\mathbf{x}_{\text{txt}}^{\text{emb}})))$

where θ^- represents the model with stopped gradient, and $d(\cdot,\cdot)$ is used to quantify the discrepancy between $f_{\theta}(\mathbf{\tilde{x}}_{\mathrm{txt}}^{\mathrm{emb}})$ and $f_{\theta^-}(\mathbf{x}_{\mathrm{txt}}^{\mathrm{emb}})$. The function \mathcal{T} serves as either the identity function or performs detokenization to generate sentences. Our objective is to preserve the robustness property of NEFTune while introducing semantic similarity through the integration of consistency between the output of noisy inputs and clean inputs. The metric function d can be any capable of measuring distance in a specific space. However, solely minimizing distance in the same embedding space might weaken the robustness effect and pose limitations on enforcing semantic similarity. In our approach, to capture textual similarity between sentences, we calculate the distance in the feature space of Sentence-BERT [40]. i.e., $d(\mathcal{T}(x), \mathcal{T}(y)) = 1 - s(\mathcal{T}(x))^{\top} s(\mathcal{T}(y)) / ||s(\mathcal{T}(x))||_1||s(\mathcal{T}(y))||_1$, where $s(\cdot)$ is the projection by using pretrained model such as SentenceBERT [40], \mathcal{T} is set to detokenization operator. We provide algorithmic descriptions of CEFT in Supplementary Material.

3.2 LMM-assisted 3D Target Volume Segmentation

For incorporating the textual information into target volume segmentation framework, we expand the concept of prompt tuning of LMM for context-aware 3D segmentation framework introduced in [35]. However, as the LMM-assisted 3D segmentation model gets the generated treatment plan as text conditions which are inevitably noisy from the previous summarization step, we introduce noise augmentation and consistency regularization modules for the target volume segmentation network, namely, Noise Embedding Segmentation (NESEG) and Regularized Consistency Embedding Segmentation (CESEG).

Noise Embedding Segmentation (NESEG). Firstly, by extending aforementioned idea of NEFTune, we inject a random noise into input data embeddings $\mathbf{x}_{\text{txt}}^{\text{emb}}$ to improve the segmentation model robustness for the generated noisy plan, and denote it as NESEG. The loss function for NESEG can be formulated as:

$$\mathcal{L}_{\text{NESEG}}(\Theta) = \mathbb{E}_{(\mathbf{x}_{\text{img}}, \tilde{\mathbf{x}}_{\text{txt}}^{\text{emb}}, \mathbf{y}_{\text{img}}) \sim D} \mathcal{L}_{\text{ce}}(g_{\psi}(\mathbf{x}_{\text{img}}; \tilde{\mathbf{y}}_{\text{txt}}^{\text{emb}}), \mathbf{y}_{\text{img}})$$
where $\tilde{\mathbf{y}}_{\text{txt}}^{\text{emb}}(\phi) = f_{\theta^*}(\tilde{\mathbf{x}}_{\text{txt}}^{\text{emb}}; \mathbf{z}_{\phi})$
(3)

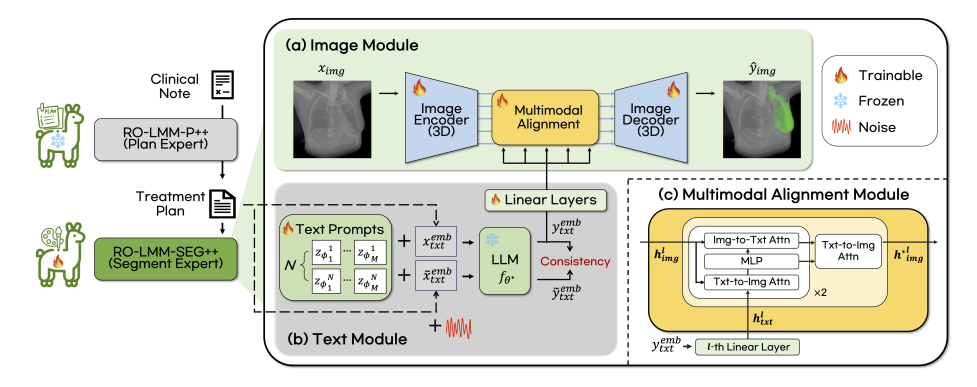


Fig. 3: Schematics of RO-LMM-SEG++ for plan-guided 3D target volume segmentation task, which composed of (a) image module and (b) text module. These module outputs are aligned through (c) multimodal alignment module.

where $\Theta = [\psi, \phi]$, $\mathbf{x}_{img} \in \mathbb{R}^{B \times HWS}$ is the 3D CT scan, B denotes batch size, H, W, and S correspond to height, width, and slice of the CT scan, $\tilde{\mathbf{y}}_{txt}^{emb} \in \mathbb{R}^{B \times 1 \times C}$ is the perturbed text embedding, $\mathbf{y}_{img} \in \mathbb{R}^{B \times HWS}$ is the 3D ground truth segmentation mask, $g_{\psi}(\cdot)$ represents the multimodal segmentation model parameterized by ψ , f_{θ^*} denotes a frozen LLM, $\tilde{\mathbf{x}}_{txt}^{emb}$ is the noise injected plan embeddings, and \mathbf{z}_{ϕ} is the learnable text prompt parametreized by ϕ . We denote this model as RO-LMM-SEG+.

Consistency Embedding Segmentation (CESEG). We further adapt the consistency regularization module for generalizing our segmentation model to both the generated noisy plan and the clean ground truth plan, and denote it as CESEG. Apart from the original concept of CEFTune, we modified the consistency regularization module for the multimodal segmentation task, which combines CEFTune and the text prompt tuning. Once the text prompt-prepended noisy embeddings of treatment plan $\tilde{\mathbf{x}}_{\mathrm{txt}}^{\mathrm{emb}}$ are inputted to the multimodal model, the output embedding is regularized with that of clean embeddings $\mathbf{x}_{\mathrm{txt}}^{\mathrm{emb}}$. The loss function for CESEG is formulated as:

$$\mathcal{L}_{\text{CESEG}}(\Theta) = \mathcal{L}_{\text{NESEG}}(\Theta) + \lambda \mathcal{R}(\phi, \phi^{-})$$
where $\mathcal{R}(\phi, \phi^{-}) = d(\tilde{\mathbf{y}}_{\text{txt}}^{\text{emb}}(\phi), \mathbf{y}_{\text{txt}}^{\text{emb}}(\phi^{-}))$ (4)

where, ϕ^- represents the learnable text prompts with stopped gradient, $d(\cdot, \cdot)$ denotes the cosine similarity, and $\mathbf{y}_{\text{txt}}^{\text{emb}} = f_{\theta^*}(\mathbf{x}_{\text{txt}}^{\text{emb}}; \mathbf{z}_{\phi^-}) \in \mathbb{R}^{B \times 1 \times C}$ is the text embedding for the clean plan $\mathbf{x}_{\text{txt}}^{\text{emb}}$. The algorithm for CESEG is provided in Supplementary Material.

The schematic of our multimodal model utilizing CESEG, denoted as RO-LMM-SEG++, is illustrated in Figure 3. We employ the 3D Residual U-Net [7] as for the backbone structure within the image module, as shown in (a). In the text module, as shown in (b), we employ pre-trained RO-LMM-P++ as for the LLM module f_{θ^*} for producing text embedding $\mathbf{y}_{\text{txt}}^{\text{emb}}$ given the treatment plan

Table 1: Details of data for training our multi-purpose RO-LMM. "US" denotes Ultrasound. "Path" indicates Pathology.

Task	Input	Output	Internal Dataset External Dataset			
	•	•	Train	Validation	Validation	
Clinical Report Summarization Treatment Plan Suggestion	MRI & US & Path Reports Clinical Note	Clinical Note Treatment Plan	5,674	60	81	
Plan-guided Target Segmentation	Treatment Plan & CT Scan	Segmentation	593	79	81	

embedding $\mathbf{x}_{\text{txt}}^{\text{emb}}$ as input. In the multimodal alignment module, as illustrated as (c), we adopt both self-attention and cross-attention mechanisms in an interactive manner (image-to-text and text-to-image) for each l-th skip-connection layer, by following the concept of promptable segmentation borrowed from Segment Anything Model (SAM) [23]). For realizing multimodal alignment within the 3D segmentation framework, we adapt the idea of light-weight text prompt tuning to transfer the linguistic capability of LLM, by following the concepts introduced in [22,35,53]. Therefore, entire parameters of the LLM module f_{θ^*} are frozen, while the learnable text prompts \mathbf{z}_{ϕ} and l-th linear layers are exclusively optimized within the text module. Further details of each module are deferred to Supplementary Material.

4 Experiments

4.1 Dataset

To train our model, we collected internal data cohort composed of 5,674 breast cancer patients treated at the Department of Radiation Oncology at Yonsei Cancer Center. For training the plan-guided 3D target volume segmentation network, we utilized multimodal data from 599 patients with their 3D CT scans and corresponding ground truth masks. To evaluate the model performance on cross-centre datasets, we further acquired external data cohort composed of 81 patients treated at the Department of Radiation Oncology at Yongin Severance Hospital. The detail of dataset is described in Table 1 and Supplementary Material. We included patients who received their initial diagnosis of breast cancer and subsequently underwent radiation therapy following curative surgery, while excluding individuals with recurrent or metastatic breast cancer in both hospitals. This study was approved by the Institutional Review Board (IRB) of each participating hospitals.

4.2 Implementation details

For instruction fine-tuning for RO-LMM-S and RO-LMM-P, we use the LLaMA-2-7B-Chat [45] model as a baseline. The maximum context length is set at 4096, and the batch size is set to 2. To train RO-LMM-SEG, we employ the 3D Residual U-Net [7] using the open-source library MONAI[†]. For incorporating the textual

[†] https://monai.io/

information within the multimodel segmentation model, we use the LLaMA-2-7B-Chat model initialized with the pre-trained checkpoint of RO-LMM-P++. We set the batch size as 1. Further details are deferred to Supplementary Material.

We use the AdamW [33] optimizer for all the tasks, with a learning rate of 5e-5 until reaching 3 epochs for both RO-LMM-S and RO-LMM-P, and 1e-4 until reaching 100 epochs for RO-LMM-SEG, leveraging 4 NVIDIA A6000 GPUs for each task. The hyper-parameter λ for CEFTune is set to 1 in all of tasks, and for consistency regularization we adopt the variants of SBERT [40] which is trained on PubMed[†] dataset, called PubMedBERT.[†]

4.3 Evaluation Metric

The evaluation of generated clinical report summaries and treatment plans utilizes common NLP metrics, including Rouge-1, Rouge-2, and Rouge-L [30]. However, acknowledging potential limitations in domain specificity for the treatment plan suggestion task, we conduct expertise-based evaluations involving two clinical experts and GPT-4.0. A board-certified expert curates a total of 5 scoring rubrics for evaluation, with detailed information available in Table S9. Using the same scoring rubrics, two clinical experts assess the performance on the plan suggestion task against ground truth labels, assigning a score of 0 or 1 for each rubric separately. Inspired by the recent evaluation methodologies such as GPT-Score [13] and G-Eval [32], GPT-4.0 also evaluates specific examples of outputs based on these rubrics with in-context learning.

To evaluate the 3D target volume segmentation performance using a ground truth segmentation mask, we measure Dice coefficient (Dice), Intersection over Union (IoU), and the 95th percentile of Hausdorff Distance (HD-95) [9] in centimeter (cm) unit to measure spatial distances between the ground truth masks and the predicted segmentation results.

To further validate effectiveness of our experiment, we provide the confidence intervals (CI) on each metric by utilizing the non-parametric bootstrap method. We calculate CI by conducting 1,000 times of random sampling procedure with replacement from the experimental results, each time equal to the total size of the sample dataset. Subsequently, we estimate the 95th percentile CI from the relative frequency distribution of each experimental trial.

4.4 Baseline Models

For text-related tasks, to validate the effectiveness of our model, we compare our model with several clinical LLMs serving as baselines, specifically MedAlpaca [14], ChatDoctor [52], Asclepius [24], and PMC-LLAMA [49]. Additionally, we include a comparison with ChatGPT [36] utilizing few-shot in-context learning for both summary and treatment plan suggestion task.

[†] https://www.ncbi.nlm.nih.gov/pubmed/

[†] https://huggingface.co/NeuML/pubmedbert-base-embeddings.

Table 2: The quantitative results for clinical note summarization using different methods. Vanilla denotes the instruction fine tuning. CI denotes confidence interval.

Model	Method	Inte	rnal Validation (N=	=60)	External Validation (N=81)			
	wicemou	Rouge 1 ↑ (CI)	Rouge 2 ↑ (CI)	Rouge L ↑ (CI)	Rouge 1 ↑ (CI)	Rouge 2 ↑(CI)	Rouge L ↑ (CI)	
Clinical Report	Summar	ization						
LLaMA2 [44]	-	0.625 (0.603-0.646)	0.439 (0.423-0.454)	0.625 (0.603-0.646)	0.667 (0.649-0.684)	0.468 (0.456-0.479)	0.667 (0.649-0.684)	
MedAlpaca [14]	-	0.529 (0.484-0.578)	0.367 (0.334-0.399)	0.529 (0.484-0.578)	0.414 (0.362-0.462)	0.329 (0.283-0.373)	0.414 (0.362-0.462)	
ChatDoctor [52]	-	0.617 (0.572-0.657)	0.411 (0.381-0.439)	0.617 (0.572-0.657)	0.549 (0.508-0.588)	0.425 (0.392-0.459)	0.549 (0.508-0.588)	
Asclepius [24]	-	0.662 (0.640-0.682)	0.447 (0.436-0.458)	0.662 (0.640-0.682)	0.590 (0.571-0.609)	0.412 (0.401-0.423)	0.590 (0.571-0.609)	
PMC-LLaMA [49]	-	0.398 (0.341-0.451)	0.239 (0.200-0.276)	0.398 (0.341-0.451)	0.382 (0.327-0.434)	0.235 (0.197-0.275)	0.382 (0.327-0.434)	
ChatGPT	-	0.672 (0.641-0.703)	0.467 (0.447-0.486)	0.672 (0.641-0.703)	0.651 (0.615-0.683)	0.456 (0.434-0.476)	0.651 (0.615-0.683)	
RO-LMM-S	Vanila	0.798 (0.777-0.818)	0.616 (0.598-0.635)	0.798 (0.777-0.818)	0.788 (0.769-0.806)	0.607 (0.586-0.628)	0.788 (0.769-0.806)	
Therapy Plan S	uggestio	ı						
LLaMA2 [44]	-	0.077 (0.071-0.083)	0.038 (0.034-0.042)	0.077 (0.071-0.083)	0.069 (0.065-0.073)	0.029 (0.027-0.031)	0.069 (0.065-0.073)	
MedAlpaca [14]	-	0.139 (0.126-0.152)	0.053 (0.049-0.058)	0.139 (0.126-0.152)	0.137 (0.123-0.152)	0.048 (0.044-0.053)	0.137 (0.123-0.152)	
ChatDoctor [52]	-	0.214 (0.194-0.234)	0.082 (0.072-0.091)	0.214 (0.194-0.234)	0.191 (0.178-0.205)	0.065 (0.060-0.071)	0.191 (0.178-0.205)	
Asclepius [24]	-	0.176 (0.162-0.190)	0.075 (0.067-0.083)	0.176 (0.162-0.190)	0.142 (0.134-0.149)	0.055 (0.051-0.059)	0.142 (0.134-0.149)	
PMC-LLaMA [49]	-	0.118 (0.101-0.137)	0.034 (0.029-0.040)	0.118 (0.101-0.137)	0.165 (0.136-0.195)	0.050 (0.040-0.060)	0.165 (0.136-0.195)	
ChatGPT	-	0.453 (0.412-0.488)	0.215 (0.187-0.246)	0.453 (0.412-0.488)	0.390 (0.357-0.423)	0.193 (0.171-0.215)	0.390 (0.357-0.423)	
RO-LMM-P	Vanila	0.651 (0.617-0.689)	0.486 (0.437-0.539)	0.651 (0.617-0.689)	0.591 (0.574-0.609)	0.426 (0.403-0.452)	0.591 (0.574-0.609)	
RO-LMM-P+	NEFT	0.639 (0.607-0.673)	0.467 (0.419-0.516)	0.639 (0.607-0.673)	0.588 (0.573-0.606)	0.419 (0.399-0.441)	0.588 (0.573-0.606)	
RO-LMM-P++	CEFT	0.668 (0.632-0.705)	0.512 (0.460-0.564)	0.668 (0.632-0.705)	0.615 (0.592-0.638)	0.459 (0.429-0.489)	0.615 (0.592-0.638)	

For the segmentation task, we utilize 3D Residual U-Net [7] and ConTEXTu-alNET [18] as our baseline methods. We further utilize an additional baseline as a variant of RO-LMM-SEG, namely LLaMA2-SEG, which is initialized with the checkpoint of vanilla LLaMA-2-7B-Chat model.

4.5 Results

Clinical Report Summarization. We present the performance of our model on the clinical report summarization task, along with confidence intervals for each method, in Table 2. Our fine-tuned model of RO-LMM-S demonstrate significant improvements over the baselines, providing consistent margins in all metrics and confidence intervals. Notably, RO-LMM-S outperforms ChatGPT with few-shot in-context learning. We also perform expert analysis on the summarized reports, and the results and experimental details are deferred to Supplementary Material.

The qualitative assessment in Table 4 further highlights the effectiveness of our proposed model, providing well-organized content and consistent formatting compared to the ground truth label. While there were minor errors observed in terms of the specific distance measurement from the nipple (red), which appears to stem from the process of integrating ultrasound and MRI images, our model accurately summarizes information in a format consistent with the provided labels. In contrast, Chat-GPT exhibits issues such as omitting essential information and generating hallucinated content (red).

Treatment Plan Suggestion. As indicated in Table 2, we evaluate the model's performance on treatment plan suggestion task based on generated clinical notes. Similar to the report summarization task, our fine-tuned variants, RO-LMM-P, exhibit substantial enhancements in suggestion performance compared to other baselines. Notably, RO-LMM-P+ shows inferior performance on the external dataset compared to the vanilla approach. However, our proposed RO-LMM-P++ achieves the best performance on both internal and external datasets across all metrics.

Table 3: Clinical expert analysis for treatment plan suggestion. R# represents each rubric and C# represents each clinical expert.

		Internal Vali	dation (N=25)		
	GPT4.0	RO-LMM-P	RO-LMM-P+ (NEFT)	RO-LMM-P++ (CEFT)	_
Experts	R1 / R2 / R3 / R4 / R5 / Total	R1 / R2 / R3 / R4 / R5 / Total	$\overline{R1 \ / \ R2 \ / \ R3 \ / \ R4 \ / \ R5 \ / \ Total}$	R1 / R2 / R3 / R4 / R5 / Total	r
C1 C2 GPT	8.8 8.4 4.4 7.2 2.0 30.8 9.6 9.6 5.6 4.4 3.8 32.7 10.0 7.6 4.8 5.6 6.8 29.2	5.6 / 10.0 / 8.8 / 9.2 / 9.2 / 42.8 5.6 / 10.0 / 8.4 / 8.8 / 9.2 / 42.0 8.2 / 8.0 / 7.2 / 8.8 / 9.6 / 37.2	5.6 / 9.6 / 8.8 / 9.2 / 9.2 / 42.4 5.6 / 9.6 / 8.0 / 8.4/ 10.0 / 41.6 9.1 / 7.6 / 6.4 / 7.6 / 9.2 / 34.8	4.8 / 10.0 / 8.8 / 9.2 / 10.0 / 42.8 4.4 / 10.0 / 8.8 / 9.2 / 9.6 / 42.0 9.1 / 8.4 / 8.0 / 8.8 / 10.0 / 39.2	0.7 0.4
			dation (N=25)		r
C1 C2 GPT	8.5 8.8 7.3 6.5 1.2 32.3 8.8 8.5 6.2 3.4 7.3 34.2 8.8 6.9 6.2 5.8 4.2 31.9	8.1 8.8 6.9 6.9 9.2 40.0 8.5 9.6 7.7 7.3 9.2 42.3 8.1 7.3 6.2 1.5 8.8 31.9	7.7 / 9.6 / 7.7 / 7.3 / 9.6 / 41.9 8.1 / 9.6 / 8.1 / 8.8 / 9.2 / 43.8 8.5 / 8.1 / 5.0 / 1.2 / 9.2 / 31.9	8.5 / 9.6 / 8.8 / 9.6 / 9.6 / 46.2 8.5 / 9.6 / 8.8 / 8.8 / 9.6 / 45.8 8.5 / 8.1 / 6.5 / 3.8 / 9.2 / 36.2	0.9 0.4

Furthermore, for the treatment plan suggestion task, we comprehensively evaluate the generated plans using our proposed expertise-based rubrics as shown in Table S9. Table 3 presents the clinical expert analysis results, where R# represents each rubric and C# represents each clinical expert. For both internal and external validation, our RO-LMM variants significantly outperform the results of GPT4.0 with few-shot in-context learning due to the specific knowledge of the domain. We confirm that our model with CEFT achieved the best performance in terms of clinical evaluation, especially on the external set, demonstrating clinical effectiveness in line with our goals. We further evaluate inter-clinicians correlation and the correlation between clinicians and GPT-4, using Pearson correlation (r). The results show strong positive correlations (> 0.7 and > 0.4, for each), affirming reliability of our proposed evaluation rubrics.

For a more detailed understanding, examples of the treatment plan suggestion task are provided in Table 4. The proposed RO-LMM-P++ (Ours) consistently yields correct answers compared to the labeled ground truth. These results demonstrate the effectiveness of our proposed CEFTune for this specific task. While Chat-GPT has shown success in providing some level of information regarding where to treat, it falls short when it comes to suggesting the specific treatment regions and dose scheme (red).

3D Target Volume Segmentation. As reported in Table 5, our proposed plan-guided 3D target segmentation frameworks excel other baseline methods with large gains, specifically remained stable performance across the external validation setting. This can be also observed in qualitative results. As shown in Figure 4(a) and (c), despite the ground truth mask posing target volume on the one side of the breast, the unimodal 3D Residual U-Net incorrectly segments contours not only the target volume but also the outside of the target breast, while all the multimodal RO-LMM variants correctly segment target volume aligning consistently with the ground truth masks. Moreover, as shown in Figure 4(a) and (b), RO-LMM-SEG+ with NESEG module yields noisy segmentation output as indicated as red arrows. RO-LMM-SEG without any proposed module shows reasonable performance, yet sometimes undersegments the treatment target volume, as shown in Figure 4(b). In contrast, our proposed RO-LMM-SEG++ with CESEG module accurately contours the breast and regional lymph nodes that need to be treated.

Table 4: Example case for the clinical report summarization task and plan suggestion task compard to baseline methods. The red scripts indicate incorrect or redundant information, and inconsistent formatting compared to the label, evaluated by a board certified clinical expert.

Clinical Repor	rt Summarization Example
User	Using the provided MRI and pathology findings, design a radiation oncologist's clinical overview. # Input: [MRI reports][Pathology reports]
Ground Truth	#1. Breast, LUM, 11:00, 4cm FN, IDC, pT1cN0M0 - Maximum diameter of invasive tumor: 1.7cm - Maximum diameter of invasive and in situ carcinoma: 1.7cm - H1N2 - LVI (-) - Intraductal carcinoma component - Proportion: 20% - Extensive intraductal component (EIC): Absent - Type: Cribriform and solid - Nuclear grade: Intermediate - Necrosis: Absent - Location: Central - Calcification: Present (Malignant) - Resection margins - Nipple, upper, outer, and inner margin: Free of carcinoma - ER/PR/Her-2/Ki-67 (90/-/2+, SISH-/11.32)
Ours	#1. Breast, LUM 11:00, 2cm FN, IDC, pT1N0M0, stage IA - T: 1.7cm (in situ 1.7cm) H1N2 - N: Total (0/5): SLN (0/4) nonSLN (0/1) - LVI (-) - Intraductal carcinoma component - Proportion: 20% - Extensive intraductal component (EIC): Absent - Type: Cribriform and solid - Nuclear grade: Intermediate - Necrosis: Absent - Location: Central -Calcification: Present (Malignant) - Resection margins - Nipple, upper, outer, and inner margin: Free of carcinoma ER/PR/HER2/Ki67: 90%/-/2+SISH-/11.32% Lum B (HER2-) type
Chat-GPT	#1 Breast, LUM, 11:00, 7cm FN, IDC, icT1N0M0, Stage IA -LUM 07:00 - Invasive ductal carcinoma - ER: 90%, PR: Negative, HER2: Equivocal (2+), Ki-67: 11.32% - Present malignant calcification - Resection margins of nipple, upper, outer, and inner margin: Free of carcinoma - Total LNs (0/5): Left sentinel No1 (0/3), left sentinel No2 (0/1), and left axillary No1 (0/1): Free of carcinoma
Treatment Pla	an Suggestion Example
User	Suggest a radiotherapy approach using the guidance from the given clinical summary of the radiation oncologist. # Input: [Clinical notes]
Ground Truth	RT to Lt. whole breast + IMN + SCL + AXL 40.05 Gy / 15 fx \rightarrow 10 Gy boost (or 48 Gy / 15 fx with IMRT).
Ours	RT to Lt. whole breast, IMN, SCL, AXL 40.05 Gy / 15 fx + 10 Gy boost (IMRT: 48 Gy / 15 fx).
Med-Alpaca	Breast, LLO 4:00 3cm FN, IDC, icT2N1M0, stage IIB \rightarrow ypT1cN1M0, stage IIA
ChatDoctor	The T-stage, N-stage, ER/PR/HER2/Ki67, and Lum A status of the tumor, as well as the patient's chemotherapy and surgical history, can all be used to determine appropriate radiation
Chat-GPT	RT to Left breast, chest wall, L axilla Conventional fractionation 40.05 Gy / 15 fx.

Table 5: Comparison of 3D target volume segmentation performance.

Model	$_{\rm LMM}$	M Internal Validation (N=79)			External Validation (N=81)			
Model .	Tuning	Dice ↑ (CI)	IoU ↑ (CI)	HD-95 ↓ (CI)	Dice ↑ (CI)	IoU ↑ (CI)	HD-95 ↓ (CI)	
3D Residual U-Net [7]	-	0.804 (0.777-0.831)	0.688 (0.653-0.720)	9.018 (7.077-11.170)	0.690 (0.652-0.725)	0.550 (0.511-0.588)	25.057 (22.844-27.070)	
ConTEXTualNET [†] [18] LLaMA2-SEG	-	0.812 (0.783-0.838) 0.817 (0.790-0.841)	0.698 (0.661-0.731) 0.705 (0.670-0.734)	7.392 (5.793-9.083) 9.101 (7.189-11.129)	0.696 (0.663-0.726) 0.692 (0.666-0.714)	0.551 (0.517-0.583) 0.539 (0.514-0.560)	21.253 (20.002-22.474) 24.087 (22.450-25.789)	
RO-LMM-SEG RO-LMM-SEG+	Vanilla NESEG	0.824 (0.799-0.846) 0.829 (0.805-0.851)	0.713 (0.680-0.742) 0.719 (0.690-0.749)	5.528 (3.978-7.295) 4.636 (3.351-6.073)	0.778 (0.743-0.806) 0.781 (0.741-0.815)	0.655 (0.621-0.686) 0.664 (0.626-0.699)	17.459 (15.254-19.678) 29.410 (27.230-31.386)	
RO-LMM-SEG++	CESEG	0.840 (0.818-0.860)	0.734 (0.706-0.760)	$4.391\ (3.227 - 5.915)$	0.766 (0.728-0.797)	0.642 (0.607-0.673)	15.236 (12.807-17.536	

Table 6: Comparison of 3D target segmentation performance between unimodal and multimodal models for both overall and specific patient types.

Types	Method	Internal Validation					External Validation			
Types	memou	#Patients	$\text{Dice} \uparrow (\text{CI})$	IoU ↑ (CI)	$\text{HD-95} \downarrow (\text{CI})$	#Patients	Dice ↑ (CI)	$IoU \uparrow (CI)$	HD-95 ↓ (CI)	
All	Unimodal Multimodal	79	0.804 (0.777-0.831) 0.840 (0.818-0.860)	0.688 (0.653-0.720) 0.734 (0.706-0.760)	9.018 (7.077-11.170) 4.391 (3.227-5.915)	81	0.690 (0.652-0.725) 0.766 (0.728-0.797)	0.550 (0.511-0.588) 0.642 (0.607-0.673)	25.057 (22.844-27.070) 15.236 (12.807-17.536)	
	Gain ↑		+0.036	+0.046	-4.627		+0.076	+0.092	-9.821	
Typical	Unimodal Multimodal	55	0.842 (0.821-0.861) 0.877 (0.866-0.888)	0.734 (0.705-0.761) 0.784 (0.766-0.802)	7.374 (5.447-9.687) 3.200 (2.361-4.303)	73	0.723 (0.694-0.749) 0.782 (0.742-0.813)	0.579 (0.546-0.610) 0.659 (0.621-0.690)	25.082 (22.783-27.380) 14.716 (12.407-17.204)	
	Gain ↑		+0.035	+0.049	-4.173		+0.059	+0.080	-10.366	
Atypica	Unimodal I Multimodal	24	0.720 (0.654-0.784) 0.760 (0.701-0.807)	0.584 (0.513-0.657) 0.628 (0.562-0.682)	12.519 (8.553-16.584) 6.948 (3.820-11.014)	8	0.370 (0.178-0.594) 0.585 (0.346-0.753)	0.259 (0.106-0.449) 0.458 (0.269-0.610)	27.138 (22.417-30.807) 22.410 (16.377-28.314)	
	Gain ↑		+0.040	+0.044	-5.571		+0.215	+0.199	-4.728	

We further categorize all patients into two distinct types: patients those who had breast-conserving surgery (typical type) and patients those who underwent

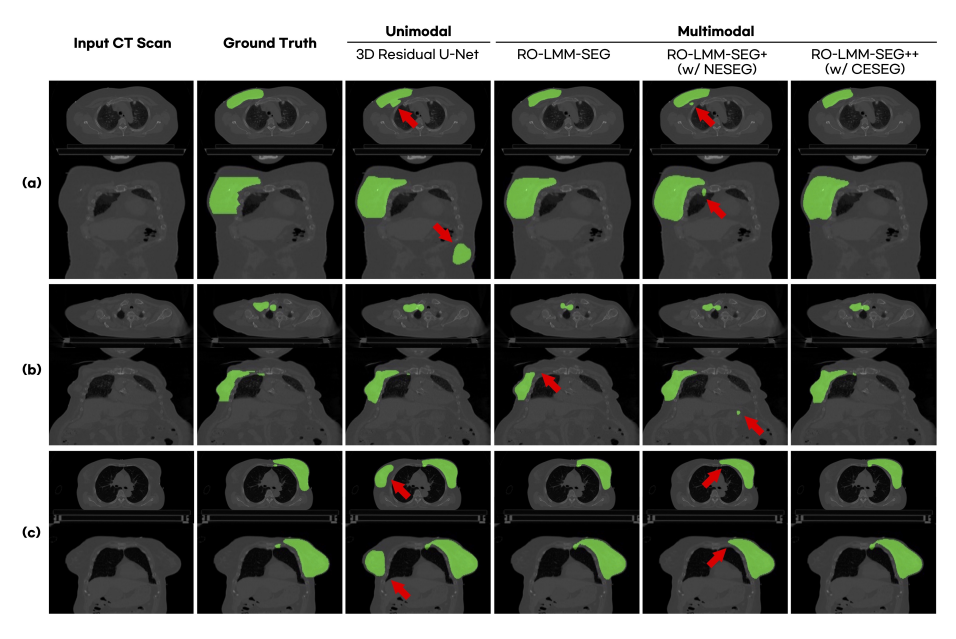


Fig. 4: Qualitative comparison on 3D target volume segmentation task between unimodal and multimodal approaches. Red arrows indicate incorrectly segmented regions.

total mastectomy (atypical type). The comparative results are presented in the Table 6 separately, with the unimodal model referred to the 3D Residual U-Net and the multimodal model denoted as our proposed RO-LMM-SEG++ with CESEG. Firstly, our proposed multimodal model shows substantial performance improvements of approximately up to 5% and 10% for internal and external validation, respectively. When comparing the typical and atypical types of patients, particularly in the less prevalent atypical type during external validation, we observed notable enhancements with a performance gain of up to 20%. This substantial generalizbility observed in extremely low-prevalence distributions demonstrates the data efficiency of our multimodal concept, leveraging textual information compared to the traditional unimodal approach.

5 Discussion

5.1 Analysis on Strategy of Separate Expert

To validate the rationale behind adopting separate strategies for each textual task, we conduct experiments by preparing a unified model shown in Table 7. We observe that the unified model's performance is significantly inferior to our distinct training strategy. This implies that summarization task, which provides information within the input, is significantly different from suggesting treatment plan that does not exist within the input, indicating the challenging nature of the

Table 7: Ablation study on adopting separate ex- Table 8: Ablation study on CEpertise for each textual task against unified strategy. SEG with input text variation for

Training Strategy	Internal $(N=60)$	External $(N=81)$		
Training Strategy	R-1 / R-2 / R-L	R-1 / R-2 / R-L		
Clinical Note Sun				
Unified strategy Distinct strategy	0.516 / 0.357 / 0.515 0.823 / 0.635 /0.822	0.327 / 0.215 / 0.326 0.805 / 0.634 / 0.804		
Therapy Plan Sug	· ' ' '			
Unified strategy Distinct strategy	$\begin{array}{c ccccccccccccccccccccccccccccccccccc$	0.409 / 0.197 / 0.406 0.606 / 0.450 / 0.606		

target segmentation performance.

		Target Segmentation			
CESEG	Input Text	Dice ↑	IoU↑		
×	Ground Truth Generated		$\begin{array}{c} 0.761_{\pm 0.103} \\ 0.714_{\pm 0.134} \end{array}$		
	$\overline{\text{Difference}\downarrow}$	0.035	0.047		
	Ground Truth Generated		$0.743_{\pm 0.111} \\ 0.733_{\pm 0.120}$		
	Difference \downarrow	0.007	0.010		

task. These results suggest that the knowledge required for each summarization and suggestion task necessitates task-aware training strategies.

Analysis on Consistency Regularization

We further analyze the effect of the proposed consistency module according to the distinct types of input text. As mentioned, the segmentation model utilizes clean ground truth data during training phase, whereas they employ noisy LMM-generated data during inference phase, potentially resulting in a performance gap. As indicated as difference in Table 8, the model's performance without our proposed consistency module significantly degrades for the generated data compared to the ground truth data for target segmentation tasks. On the other hand, employing our proposed CESEG ensures robust performance for the generated data compared to ground truth data. In particular, our model exhibits a performance difference between two distinct input data of less than 1%. The results indicate that our key idea of consistency module effectively alleviates performance degradation when using LMM-generated data as input.

5.3 Limitation

While our study provides valuable insights on the application of radiation oncology, there are several limitations to consider. Firstly, the dataset used in this study is currently confined to patients with their initial diagnoses, primarily focusing on breast cancer. Expanding the scope of our research to include diverse patient scenarios and other cancer types is essential for enhancing the applicability of our model. Secondly, achieving detailed target volume segmentation for Simultaneous Integrated Boost (SIB) necessitates information beyond treatment plan-guided segmentation. This additional information may be obtained from alternative imaging modalities, such as MRI or PET-CT, along with ground truth masks for organ-at-risks (OARs) and gross tumor volume (GTV). Consequently, SIB is excluded from this study. Future research will focus on developing a model for SIB by incorporating a more extensive array of information.

6 Conclusion

In this work, we introduce RO-LMM, a multi-purpose foundation model tailored for radiation oncology. Addressing limitations in current medical AI models confined to specific tasks, RO-LMM demonstrates proficiency in diverse tasks: clinical report summarization, radiation treatment plan suggestion, and plan-guided 3D target volume segmentation, mirroring real-world clinical workflows. Another key contribution of this work is the introduction of consistency technique into both text and segmentation task. Results from multi-center cohort datasets confirm RO-LMM's promising performance and noteworthy generalization capabilities across diverse tasks. These findings mark a significant stride toward developing a versatile AI model, hinting at the potential for a multi-purpose medical AI model in radiation oncology.

Ethical Statement All the patient information and any potential personally identifiable information from used datasets are de-identified, and clinical data usage is approved by the Institutional Review Board (IRB).

References

- Aghajanyan, A., Shrivastava, A., Gupta, A., Goyal, N., Zettlemoyer, L., Gupta, S.: Better fine-tuning by reducing representational collapse. arXiv preprint arXiv:2008.03156 (2020)
- Brown, T., Mann, B., Ryder, N., Subbiah, M., Kaplan, J.D., Dhariwal, P., Nee-lakantan, A., Shyam, P., Sastry, G., Askell, A., et al.: Language models are few-shot learners. Advances in neural information processing systems 33, 1877–1901 (2020)
- 3. Bubeck, S., Chandrasekaran, V., Eldan, R., Gehrke, J., Horvitz, E., Kamar, E., Lee, P., Lee, Y.T., Li, Y., Lundberg, S., et al.: Sparks of artificial general intelligence: Early experiments with gpt-4. arXiv preprint arXiv:2303.12712 (2023)
- Chiang, W.L., Li, Z., Lin, Z., Sheng, Y., Wu, Z., Zhang, H., Zheng, L., Zhuang, S., Zhuang, Y., Gonzalez, J.E., et al.: Vicuna: An open-source chatbot impressing gpt-4 with 90%* chatgpt quality. See https://vicuna. lmsys. org (accessed 14 April 2023) (2023)
- Choi, M.S., Choi, B.S., Chung, S.Y., Kim, N., Chun, J., Kim, Y.B., Chang, J.S., Kim, J.S.: Clinical evaluation of atlas-and deep learning-based automatic segmentation of multiple organs and clinical target volumes for breast cancer. Radiotherapy and Oncology 153, 139–145 (2020)
- Chung, S.Y., Chang, J.S., Choi, M.S., Chang, Y., Choi, B.S., Chun, J., Keum, K.C., Kim, J.S., Kim, Y.B.: Clinical feasibility of deep learning-based auto-segmentation of target volumes and organs-at-risk in breast cancer patients after breast-conserving surgery. Radiation Oncology 16(1), 1–10 (2021)
- Çiçek, Ö., Abdulkadir, A., Lienkamp, S.S., Brox, T., Ronneberger, O.: 3d u-net: learning dense volumetric segmentation from sparse annotation. In: Medical Image Computing and Computer-Assisted Intervention-MICCAI 2016: 19th International Conference, Athens, Greece, October 17-21, 2016, Proceedings, Part II 19. pp. 424-432. Springer (2016)

- 8. Conover, M., Hayes, M., Mathur, A., Xie, J., Wan, J., Shah, S., Ghodsi, A., Wendell, P., Zaharia, M., Xin, R.: Free dolly: Introducing the world's first truly open instruction-tuned llm (2023), https://www.databricks.com/blog/2023/04/12/dolly-first-open-commercially-viable-instruction-tuned-llm
- Crum, W.R., Camara, O., Hill, D.L.: Generalized overlap measures for evaluation and validation in medical image analysis. IEEE transactions on medical imaging 25(11), 1451–1461 (2006)
- Dai, W., Li, J., Li, D., Tiong, A.M.H., Zhao, J., Wang, W., Li, B., Fung, P., Hoi, S.: Instructblip: Towards general-purpose vision-language models with instruction tuning (2023)
- 11. Ding, Z., Wang, J., Tu, Z.: Open-vocabulary universal image segmentation with maskelip (2023)
- Driess, D., Xia, F., Sajjadi, M.S.M., Lynch, C., Chowdhery, A., Ichter, B., Wahid, A., Tompson, J., Vuong, Q., Yu, T., Huang, W., Chebotar, Y., Sermanet, P., Duckworth, D., Levine, S., Vanhoucke, V., Hausman, K., Toussaint, M., Greff, K., Zeng, A., Mordatch, I., Florence, P.: Palm-e: An embodied multimodal language model (2023)
- 13. Fu, J., Ng, S.K., Jiang, Z., Liu, P.: Gptscore: Evaluate as you desire. arXiv preprint arXiv:2302.04166 (2023)
- Han, T., Adams, L.C., Papaioannou, J.M., Grundmann, P., Oberhauser, T., Löser, A., Truhn, D., Bressem, K.K.: Medalpaca-an open-source collection of medical conversational ai models and training data. arXiv preprint arXiv:2304.08247 (2023)
- Hosny, A., Parmar, C., Quackenbush, J., Schwartz, L.H., Aerts, H.J.: Artificial intelligence in radiology. Nature Reviews Cancer 18(8), 500–510 (2018)
- Hu, E.J., Shen, Y., Wallis, P., Allen-Zhu, Z., Li, Y., Wang, S., Wang, L., Chen, W.: Lora: Low-rank adaptation of large language models (2021)
- 17. Hua, H., Li, X., Dou, D., Xu, C.Z., Luo, J.: Noise stability regularization for improving bert fine-tuning. arXiv preprint arXiv:2107.04835 (2021)
- Huemann, Z., Hu, J., Bradshaw, T.: Contextual net: A multimodal vision-language model for segmentation of pneumothorax. arXiv preprint arXiv:2303.01615 (2023)
- 19. Jain, N., Chiang, P.y., Wen, Y., Kirchenbauer, J., Chu, H.M., Somepalli, G., Bartoldson, B.R., Kailkhura, B., Schwarzschild, A., Saha, A., et al.: Neftune: Noisy embeddings improve instruction finetuning. arXiv preprint arXiv:2310.05914 (2023)
- 20. Jiang, H., He, P., Chen, W., Liu, X., Gao, J., Zhao, T.: Smart: Robust and efficient fine-tuning for pre-trained natural language models through principled regularized optimization. arXiv preprint arXiv:1911.03437 (2019)
- 21. Joshi, G., Jain, A., Adhikari, S., Garg, H., Bhandari, M.: Fda approved artificial intelligence and machine learning (ai/ml)-enabled medical devices: An updated 2022 landscape. medRxiv pp. 2022–12 (2022)
- 22. Kim, K., Oh, Y., Ye, J.C.: Zegot: Zero-shot segmentation through optimal transport of text prompts. arXiv preprint arXiv:2301.12171 (2023)
- 23. Kirillov, A., Mintun, E., Ravi, N., Mao, H., Rolland, C., Gustafson, L., Xiao, T., Whitehead, S., Berg, A.C., Lo, W.Y., et al.: Segment anything. arXiv preprint arXiv:2304.02643 (2023)
- Kweon, S., Kim, J., Kim, J., Im, S., Cho, E., Bae, S., Oh, J., Lee, G., Moon, J.H., You, S.C., et al.: Publicly shareable clinical large language model built on synthetic clinical notes. arXiv preprint arXiv:2309.00237 (2023)
- 25. Lai, X., Tian, Z., Chen, Y., Li, Y., Yuan, Y., Liu, S., Jia, J.: Lisa: Reasoning segmentation via large language model. arXiv preprint arXiv:2308.00692 (2023)
- 26. Li, B., Weinberger, K.Q., Belongie, S., Koltun, V., Ranftl, R.: Language-driven semantic segmentation. arXiv preprint arXiv:2201.03546 (2022)

- 27. Li, J., Li, D., Savarese, S., Hoi, S.: Blip-2: Bootstrapping language-image pre-training with frozen image encoders and large language models (2023)
- Li, Z., Li, Y., Li, Q., Wang, P., Guo, D., Lu, L., Jin, D., Zhang, Y., Hong, Q.: Lvit: Language meets vision transformer in medical image segmentation. IEEE Transactions on Medical Imaging pp. 1–1 (2023). https://doi.org/10.1109/TMI. 2023.3291719
- Liang, F., Wu, B., Dai, X., Li, K., Zhao, Y., Zhang, H., Zhang, P., Vajda, P., Marculescu, D.: Open-vocabulary semantic segmentation with mask-adapted clip (2023)
- 30. Lin, C.Y.: Rouge: A package for automatic evaluation of summaries. In: Text summarization branches out. pp. 74–81 (2004)
- 31. Liu, H., Li, C., Wu, Q., Lee, Y.J.: Visual instruction tuning. arXiv preprint arXiv:2304.08485 (2023)
- 32. Liu, Y., Iter, D., Xu, Y., Wang, S., Xu, R., Zhu, C.: G-eval: Nlg evaluation using gpt-4 with better human alignment, may 2023. arXiv preprint arXiv:2303.16634
- 33. Loshchilov, I., Hutter, F.: Decoupled weight decay regularization. arXiv preprint arXiv:1711.05101 (2017)
- 34. Moor, M., Banerjee, O., Abad, Z.S.H., Krumholz, H.M., Leskovec, J., Topol, E.J., Rajpurkar, P.: Foundation models for generalist medical artificial intelligence. Nature **616**(7956), 259–265 (2023)
- 35. Oh, Y., Park, S., Byun, H.K., Kim, J.S., Ye, J.C.: Llm-driven multimodal target volume contouring in radiation oncology (2023)
- 36. OpenAI: Chatgpt. OpenAI Blog (2021)
- OpenAI: Gpt-4 technical report. ArXiv abs/2303.08774 (2023), https://api.semanticscholar.org/CorpusID:257532815
- Ouyang, L., Wu, J., Jiang, X., Almeida, D., Wainwright, C.L., Mishkin, P., Zhang, C., Agarwal, S., Slama, K., Ray, A., et al.: Training language models to follow instructions with human feedback, 2022. URL https://arxiv.org/abs/2203.02155 13 (2022)
- Rajpurkar, P., Lungren, M.P.: The current and future state of ai interpretation of medical images. New England Journal of Medicine 388(21), 1981–1990 (2023)
- 40. Reimers, N., Gurevych, I.: Sentence-bert: Sentence embeddings using siamese bert-networks. arXiv preprint arXiv:1908.10084 (2019)
- 41. Singhal, K., Azizi, S., Tu, T., Mahdavi, S.S., Wei, J., Chung, H.W., Scales, N., Tanwani, A., Cole-Lewis, H., Pfohl, S., et al.: Large language models encode clinical knowledge. arXiv preprint arXiv:2212.13138 (2022)
- 42. Taori, R., Gulrajani, I., Zhang, T., Dubois, Y., Li, X., Guestrin, C., Liang, P., Hashimoto, T.B.: Stanford alpaca: An instruction-following llama model (2023)
- 43. Touvron, H., Lavril, T., Izacard, G., Martinet, X., Lachaux, M.A., Lacroix, T., Rozière, B., Goyal, N., Hambro, E., Azhar, F., et al.: Llama: Open and efficient foundation language models. arXiv preprint arXiv:2302.13971 (2023)
- 44. Touvron, H., Martin, L., Stone, K., Albert, P., Almahairi, A., Babaei, Y., Bashlykov, N., Batra, S., Bhargava, P., Bhosale, S., et al.: Llama 2: Open foundation and fine-tuned chat models. arXiv preprint arXiv:2307.09288 (2023)
- Touvron, H., Martin, L., Stone, K., Albert, P., Almahairi, A., Babaei, Y., Bashlykov, N., Batra, S., Bhargava, P., Bhosale, S., et al.: Llama 2: Open foundation and fine-tuned chat models. arXiv preprint arXiv:2307.09288 (2023)
- Tu, T., Azizi, S., Driess, D., Schaekermann, M., Amin, M., Chang, P.C., Carroll, A., Lau, C., Tanno, R., Ktena, I., et al.: Towards generalist biomedical ai. arXiv preprint arXiv:2307.14334 (2023)

- Wang, Y., Kordi, Y., Mishra, S., Liu, A., Smith, N.A., Khashabi, D., Hajishirzi,
 H.: Self-instruct: Aligning language model with self generated instructions. arXiv
 preprint arXiv:2212.10560 (2022)
- 48. Wang, Z., Lu, Y., Li, Q., Tao, X., Guo, Y., Gong, M., Liu, T.: Cris: Clip-driven referring image segmentation. In: Proceedings of the IEEE/CVF conference on computer vision and pattern recognition. pp. 11686–11695 (2022)
- 49. Wu, C., Zhang, X., Zhang, Y., Wang, Y., Xie, W.: Pmc-llama: Further finetuning llama on medical papers. arXiv preprint arXiv:2304.14454 (2023)
- 50. Wu, C., Zhang, X., Zhang, Y., Wang, Y., Xie, W.: Towards generalist foundation model for radiology. arXiv preprint arXiv:2308.02463 (2023)
- 51. Yun, S., Park, S.H., Seo, P.H., Shin, J.: Ifseg: Image-free semantic segmentation via vision-language model (2023)
- 52. Yunxiang, L., Zihan, L., Kai, Z., Ruilong, D., You, Z.: Chatdoctor: A medical chat model fine-tuned on llama model using medical domain knowledge. arXiv preprint arXiv:2303.14070 (2023)
- 53. Zhou, K., Yang, J., Loy, C.C., Liu, Z.: Conditional prompt learning for vision-language models (2022)
- 54. Zhu, C., Cheng, Y., Gan, Z., Sun, S., Goldstein, T., Liu, J.: Freelb: Enhanced adversarial training for natural language understanding. arXiv preprint arXiv:1909.11764 (2019)

A Supplementary Section

In this supplemental documents, we present:

- An algorithmic descriptions of our proposed Consistency Embedding Fine Tuning (CEFT) and Consistency Embedding Segmentation (CESEG) in Section B.
- An explanation of the network architecture for the segmentation model in Section C.
- Results of ablation studies for both text-related tasks and target volume segmentation tasks in Section D and Section C.
- Detailed information about the dataset, including pre-processing and acquisition procedures, in Section F.
- Examples of the entire workflow in Section I.
- Additional comparison results for all tasks in Section G.
- Detailed descriptions of the evaluation for treatment plan suggestion, including prompts for evaluation, in Section J.
- Detailed descriptions of the expert-analysis for clinical report summarization, including prompts for evaluation, in Section H.

B Algorithm of CEFTune and CESEG

Algorithm 1 and Algorithm 2 details the training procedure with CEFTune and CESEG, respectively.

```
Algorithm 1: CEFTune: Consistency Embedding Fine tuning
```

```
Input: \{X_i^{\text{txt}}, Y_i^{\text{txt}}\}_{i=1}^N \sim D tokenized dataset, large language model f_{\theta}(\cdot),
                           detokenization operator \mathcal{T}(\cdot), the metric which calculate the cosine
                           similarly d(\cdot, \cdot), the hyper-parameter for the noise intensity and loss,
                           \alpha, and \lambda, repectively. The cross entropy loss \mathcal{L}_{ce},
                           the embedding layer emb(·), \theta^- \leftarrow \text{stopgrad } (\theta);
1 repeat
             Sample (\mathbf{x}_{\text{txt}}, \mathbf{y}_{\text{txt}}) \sim D;
\mathbf{2}
             \mathbf{x}_{\mathrm{txt}}^{\mathrm{emb}} \leftarrow \mathrm{emb}(\mathbf{x}_{\mathrm{txt}});
3
             \hat{\mathbf{y}}_{\text{txt}} \leftarrow f_{\theta^{-}}(\mathbf{x}_{\text{txt}}^{\text{emb}}) ;
4
              \epsilon \sim \mathcal{U}(-1,1);
             \tilde{\mathbf{x}}_{\mathrm{txt}}^{\mathrm{emb}} \leftarrow \mathbf{x}_{\mathrm{txt}}^{\mathrm{emb}} + (\alpha/\sqrt{LC})\epsilon;
             \tilde{\mathbf{y}}_{\mathrm{txt}} \leftarrow f_{\theta}(\tilde{\mathbf{x}}_{\mathrm{txt}}^{\mathrm{emb}}) ;
             \mathcal{L}(\theta) \leftarrow \mathcal{L}_{ce}(\mathbf{\hat{y}}_{txt}, \mathbf{y}_{txt}) + \lambda d(\mathcal{T}(\mathbf{\tilde{y}}_{txt}), \mathcal{T}(\mathbf{\hat{y}}_{txt}))
9 until Stopping criteria met max iterations;
```

 $\mathbf{2}$

3

4

5

Algorithm 2: CESEG: Consistency Embedding Segmentation

: $\{X_i^{\text{img}}, X_i^{\text{txt}}, Y_i^{\text{img}}\}_{i=1}^M \sim D$, the entire image segmentation model $g_{\Theta}(\cdot)$, where $\Theta = [\psi, \phi]$, which consist of segmentation model g_{ψ} , and learnable text prompt z_{ϕ} . The frozen large language model $f_{\theta^*}(\cdot)$, output embedding of f_{θ^*} $\mathbf{y}_{\mathrm{txt}}^{\mathrm{emb}}$, the hyper-parameter for the noise intensity and loss α and λ , respectively, the metric which calculate the cosine similarity $d(\cdot,\cdot)$, the cross entropy loss \mathcal{L}_{ce} , the embedding layer emb(·), $\phi^- \leftarrow \text{stopgrad } (\phi)$, 1 repeat Sample $(\mathbf{x}_{img}, \mathbf{x}_{txt}, \mathbf{y}_{img}) \sim D$; $\mathbf{x}_{\mathrm{txt}}^{\mathrm{emb}} \leftarrow \mathrm{emb}(\mathbf{x}_{\mathrm{txt}})$; $\mathbf{y}_{\mathrm{txt}}^{\mathrm{emb}} \leftarrow f_{\theta^*}(\mathbf{x}_{\mathrm{txt}}^{\mathrm{emb}}; \mathbf{z}_{\phi}) ;$ $\epsilon \sim \mathcal{U}(-1,1);$

 $\begin{aligned} & \mathbf{\tilde{x}}_{\text{txt}}^{\text{emb}} \leftarrow \mathbf{x}_{\text{txt}}^{\text{emb}} + (\alpha/\sqrt{LC})\epsilon \ ; \\ & \mathbf{\tilde{y}}_{\text{txt}}^{\text{emb}} \leftarrow f_{\theta^*}(\mathbf{\tilde{x}}_{\text{txt}}^{\text{emb}}; \mathbf{z}_{\phi^-}) \ ; \end{aligned}$ $\mathcal{L}(\Theta) \leftarrow \mathcal{L}_{\text{ce}}(g_{\psi}(\mathbf{x}_{\text{img}}; \mathbf{\tilde{y}}_{\text{txt}}^{\text{emb}}), \mathbf{y}_{\text{img}}) + \lambda d(\mathbf{\tilde{y}}_{\text{txt}}^{\text{emb}}, \mathbf{y}_{\text{txt}}^{\text{emb}})$

9 until Stopping criteria met max iterations;

\mathbf{C} Architecture of RO-LMM-SEG++

The schematic of our RO-LMM-SEG++ is illustrated in Figure 3. For text prompt tuning of LLM, we introduce a total of N-text prompts $\{\mathbf{z}_{\phi}^{n}|_{n=1}^{N}\}$, where each $\mathbf{z}_{\phi}^{n} \in \mathbb{R}^{M \times C}$ is composed of M vectors with the dimension C. These learnable vectors are randomly initialized, and then consistently prepended to each of treatment plan embedding $\mathbf{x}_{\mathrm{txt}}^{\mathrm{emb}} \in \mathbb{R}^{B \times L \times C}$. Here, the final prompted text input t can be formulated as follows:

$$t = \{\mathbf{z}_{\phi_1}^n, \mathbf{z}_{\phi_2}^n, ..., \mathbf{z}_{\phi_M}^n, \mathbf{x}_{\text{txt}}^{\text{emb}}\}.$$
 (5)

Then, using the prompted text input t, the frozen LLM resulted the text embedding $\mathbf{y}_{\text{txt}}^{\text{emb}} \in \mathbb{R}^{B \times 1 \times C}$ as for the last token output. Then, to align the text embedding with the intermediate image embedding $h_{img}^l \in \mathbb{R}^{B \times H_l W_l S_l \times Ch_l}$, $\mathbf{y}_{\mathrm{txt}}^{\mathrm{emb}}$ is projected to yield $h_{txt}^l \in \mathbb{R}^{B \times 1 \times Ch_l}$ via l-th layer-wise linear layer, where H_l , W_l , and S_l correspond to height, width, and slice of the image embedding, and Ch_l is the channel dimension of l-th skip-connection layer within the image module. For multimodal alignment, the projected text embeddings h_{txt}^l is selfattended and crossly-attended with the image embedding h_{imq}^l for each layer, and each multimodal embedding h^{*l}_{img} is inputted to the decoder part of the image module to yield final prediction $\hat{y}_{\text{img}} \in \mathbb{R}^{B \times 1 \times HWS}$.

D Ablation Study on Therapy Plan Suggestion

To investigate the effectiveness of our proposed methods, we conduct the ablation studies for treatment plan suggestion task, as shown in Table S1.

Component	Condition	Ours	Internal	Validatio	n (N=60)	External	Validatio	n (N=81)	
Component	Condition	Ours	Rouge 1 ↑	Rouge 2 ↑	Rouge L ↑	Rouge 1 ↑	Rouge 2 ↑	Rouge L↑	
Teacher Module	Noisy teacher Clean teacher	✓	0.613 0.652	0.453 0.491	0.615 0.649	0.575 0.606	0.428 0.450	0.571 0.604	
SBERT Moudle	SBERT PubMedBERT	√	0.648 0.652	0.484 0.491	0.645 0. 649	0.598 0.606	0.442 0.450	0.594 0.604	
Noise Intensity (α)	5 10 15	✓	0.652 0.648 0.642	0.491 0.488 0.481	0.649 0.647 0.642	0.606 0.597 0.576	0.450 0.435 0.415	0.604 0.598 0.572	
Noise type	Uniform 5 Gaussian 5	✓	0.652 0.625	0.491 0.449	0.649 0.629	0.606 0.588	0.450 0.425	0.604 0.586	
Backbone	LLaMA-13B +NEFT + CEFT	√	0.645 0.658 0.662	0.478 0.500 0.502	0.640 0.653 0.661	0.597 0.601 0.613	0.436 0.438 0.441	0.594 0.597 0.603	
Temperature	0.6 0.8	✓	0.647 0.652	0.480 0.491	0.643 0.649	0.593 0.606	0.435 0.450	0.591 0.604	

Table S1: Component analysis of RO-LMM-P framework on treatment plan suggestion.

Consistency Regularization Loss We manipulate the objective function in Equation 3 to analyze the effect of consistency regularization. By default, we use $f_{\theta^-}(\mathbf{x}_{\text{txt}}^{\text{emb}})$ as the target (referred to as "clean teacher"). For comparison, we set $f_{\theta^-}(\mathbf{\tilde{x}}_{\text{txt}}^{\text{emb}})$ as the teacher and $f_{\theta}(\mathbf{x}_{\text{txt}}^{\text{emb}})$ as the student (referred to as "noisy teacher"). We observe that the clean teacher significantly outperforms the noisy teacher. By restricting the divergence of the distribution of students, the clean teacher yields enhanced performance compared to the noisy teacher.

Effect of SBERT Module We study the effect of the SBERT module in enforcing consistency between clean and noisy input. Our model, equipped with the medical domain-specific SBERT variant, PubMedBERT, outperforms models trained on general language. This demonstrates the effectiveness of incorporating domain-specific knowledge.

Analysis of Noise type and Intensity (α) Since our proposed method involves injecting noise into embeddings, we conduct a study to analyze the effect of noise type and intensity under various conditions. First, regarding the noise type, we found that our method performed best when equipped with uniform noise compared to Gaussian noise. Consequently, we set the default configuration for noise type to uniform noise. Additionally, we analyze the effect of noise intensity by varying the parameter α from 5 to 15. Smaller values of α resulted in better performance on the internal dataset, while larger values improved performance on the external dataset. However, excessively large values of α led to a significant drop in performance on the external dataset. Based on empirical results, we select α set to 5 as the baseline.

Analysis of Model Backbone We conduct experiments using the larger 13B LLaMA-2 backbone version and observ a similar performance trend compared to the 7B model. Despite the larger backbone size, our proposed CEFT method outperform the other baselines, demonstrating scalability. Taking into account both cost-effectiveness and performance, we adopt the 7B model as the default configuration.

Analysis of Temperature To investigate the impact of stochasticity, we conducted experiments varying the temperature during treatment plan suggestion generation. Our findings indicate that the results produced by our proposed method are insensitive and robust to changes in temperature. Based on empirical analysis, we set the default temperature to 0.8.

E Ablation Study on Target Segmentation

To optimize treatment target segmentation performance, we conduct the ablation studies, as shown in Table S2.

Analysis of LMM Tuning Methods We compare the different LMM tuning methods to find optimal performance, where NESEG nor CESEG module is not activated. We analyze various methods including no tuning, low-rank adaptation (LoRA) fine-tuning [16] and prompt tuning methods with a single or multiple text prompts. From the experimental results, the text prompt tuning shows the most reliable performance across the external validation setting. Additionally, the use of single text prompt shows a remarkable improvement in performance compared to utilizing multiple text prompts.

Analysis of Noise Intensity (α) We analyze the effect of noise intensity by varying α from 5 to 20, where CESEG module is not activated. We empirically find that α as 10 yields the best performance. We further train the hyper-parameter α as a learnable parameter, however, yielding inferior performance compared to employing the fixed noise.

Table S2: Component analysis of RO-LMM-SEG framework on target volume segmentation performance.

Component	Condition	Ours	Internal	Validation (N=79)		External	External Validation (N=81)			
component	Condition	ours	Dice ↑	IoU ↑	HD-95 ↓	Dice ↑	IoU ↑	HD-95 ↓		
	None		0.822	0.712	12.368	0.752	0.622	24.849		
	LoRA [16]		0.810	0.699	4.989	0.759	0.637	16.692		
LMM Tuning Method	Text Prompts (p=1)	✓	0.825	0.714	5.392	0.775	0.652	17.623		
	Text Prompts (p=2)		0.822	0.711	7.030	0.757	0.627	24.64		
	5		0.821	0.707	5.917	0.738	0.601	22.320		
Noise Intensity (α)	10	✓	0.830	0.720	4.383	0.771	0.653	28.835		
	20		0.826	0.716	5.575	0.732	0.593	26.090		
	Learnable		0.828	0.715	5.024	0.757	0.633	23.694		

F Details of Training Dataset

For data preparation, we collected internal training & validation data from patients treated at Yonsei Cancer Center between January 2009 and December 2022. For external validation, we further collected data from patients from Yongin Severance Hospital between January 2018 and December 2022. We confirmed that the external test set was not overlapped with the training dataset.

For pre-processing image data for training RO-LMM-SEG++, all the 3D chest CT scans and target volumes were re-sampled with identical voxel spacing of 1.0 \times 1.0 \times 3.0 mm³. The intensity values of the CT scans were truncated between -1,000 and 1,000 of Hounsfield unit (HU), and linearly normalized between 0 and 1.0. When training, a 3D patch with a spatial dimension of 384 \times 384 \times 128 pixels was randomly cropped. When inference, the entire 3D CT scans was tested using sliding windows with the identical spatial dimension of the 3D patch to that used for training.

G Additional Qualitative Results

In this section, we provide the additional qualitative results on all tasks as shown in Table S4, Table S5 and Figure S1.

In the context of report summarization task involving cases with multiple (two or more) tumor masses, as shown in in Table S4, our model adeptly summarize the existence of two tumors in the first line of the summary, despite minor inaccuracies in pinpointing the exact locations of the tumors. In contrast, ChatGPT incorrectly summarize these cases as having only one tumor mass in the first line. Additionally, ChatGPT exhibit instances of hallucination, such as inappropriately mentioning tumor sizes in the first line, erroneously including post-therapy (yp) stages for patients who did not receive chemotherapy, and excessively condensing key information such as the presence of the lymph node metastasis, making it challenging to discern. Overall, unlike our model which aligns closely with the ground truth in its summaries, ChatGPT demonstrates significant issues, including the generation of erroneous hallucination and the failure to comprehensively encapsulate necessary details.

In the evaluation of treatment plan suggestion capabilities in Table S5, only our model and ChatGPT are able to offer somewhat meaningful suggestions related to radiotherapy treatment, while other models fail. ChatGPT, drawing upon its built-in knowledge base, seems to propose plans that are partially relevant. However, it exhibited a fundamental misunderstanding of dose schemes, frequently misinterpreting hypofractionation as conventional fractionation. A significant limitation in ChatGPT's approach is its inability to incorporate all regional lymph node areas into the target volume, often disproportionately focusing on specific areas, such as the axillary lymph nodes. Additionally, ChatGPT struggles to distinguish between the treatment of the breast and the chest wall, leading to flawed treatment plan suggestions. These limitations seen to arise from ChatGPT's lack of a holistic understanding of radiation oncology, unlike our domain-specific model.

Figure S1 provides qualitative comparisons of the target volume segmentation performance for breast cancer patients, where the unimodal model fails to segment target volume with incorrect laterality as indicated as red arrows. On the other hand, our proposed multimodal RO-LMM-SEG++ with CESEG shows the most promising qualitative segmentation performance, aligning consistently with the ground truth masks.

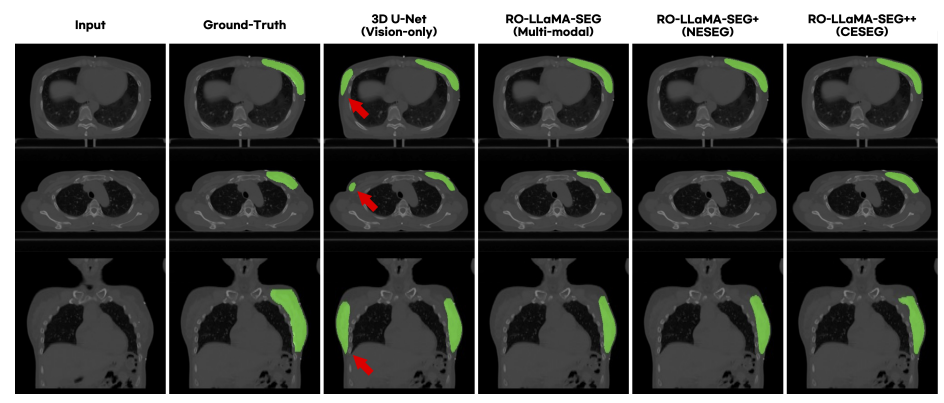


Fig. S1: 3D target volume segmentation cases compared to baseline methods. Red arrows indicate incorrectly segmented regions.

H Expert Analysis on Clinical Report Summarization

Similar to treatment plan suggestions, we evaluate the generated summaries using our proposed expertise-based rubrics, as illustrated in Tab. S9, and compare them with other baselines, including ChatGPT and LLaMa-2. Tab. S3 presents the results of clinical expert analysis, where R# represents each rubric and C# represents each clinical expert. For both internal and external validation, our ROB-LMM-S significantly outperforms all other baselines due to its specific knowledge in this domain. We further evaluate inter-clinician correlation using Pearson correlation (r), with results showing strong positive correlations (> 0.85 and > 0.95, for each internal and external validation), affirming the reliability of our proposed evaluation rubrics and the clinical effectiveness of our ROB-LMM-S. Therefore, our ROB-LMM-S provides practical and meaningful summaries that can assist in the field of radiation oncology.

Table S3: Clinical expert analysis for Clinical report summarization. R# represents each rubric and C# represents each clinical expert.

	Internal Validation (N=10)											
	GPT	LLaMa2-7B	RO-LMM-S									
Experts	8 R1 / R2 / R3 / R4 / Total	$\overline{R1~/~R2~/~R3~/~R4~/~Total}$	R1 / R2 / R3 / R4 / Total	r								
C1 C2	$\begin{matrix} 3.0 & / & 0.0 & / & 4.0 & / & 7.0 & / & 13.3 \\ 3.0 & / & 0.0 & / & 5.0 & / & 7.0 & / & 14.4 \end{matrix}$	$ \frac{2.0 \mid 0.0 \mid 0.0 \mid 7.0 \mid 9.0}{1.0 \mid 0.0 \mid 0.0 \mid 9.0 \mid 10.0} $	$15.0 \ / \ 10.0 \ / \ 10.0 \ / \ 10.0 \ / \ 45.0 \ 15.0 \ / \ 10.0 \ / \ 9.0 \ / \ 10.0 \ / \ 44.0$).88								
		External Validation (N=	=10)	r								
C1 C2		7.0 / 0.0 / 0.0 / 7.0 / 14.0 8.0 / 0.0 / 0.0 / 9.0 / 17.0	10.0 / 9.0 / 8.0 / 8.0 / 35.0 10.0 / 9.0 / 8.0 / 9.0 / 36.0).97								

Table S4: Example case for the clinical report summarization task. The **red** scripts indicate the incorrect or redundant information, and inconsistent format compared to label.

User	Using the provided MRI and pathology findings, design a radiation oncologist's clinical overview. ## Input: [MRI report] [Pathology report]
Ground truth	# 1. Breast, RLO 08:00 4cm FN, RLM 04:00 2cm FN, IDC, two, pT1cN1aM0, stage IIA - Histologic type: Invasive ductal carcinoma, NOS - Tumor margin: Infiltrative - Maximum diameter of invasive tumor: 1.5cm and 0.4cm - Maximum diameter of invasive and in situ carcinoma: 3.0cm - Nuclear grade: 2 - Histologic grade: II (3-2-1) - LVI (-) PNI (-) - Intraductal carcinoma component - Proportion: 10% - Extensive intraductal component (EIC): Absent - Type: Cribriform - Nuclear grade: Low - Necrosis: Absent - Location: Periphery - Calcification: Present (Malignant abd benign) - Associated benign lesion: Intraductal papilloma, sclerosing adenosis and columnar cell lesion - RM (-) - Overlying skin (superficial margin): Free of ca (safety margin: 1.4cm) - Underlying fascia (deep margin): Free of ca (safety margin: 2.3cm) - Lymph nodes, total (2/13): PNE (-, Maximal diameter: 3mm) - Axillary (0/10): Free of ca - Sentinel lymph node1 (1/1), axillary lymph node1 (1/1), axillary lymph node2 (0/1) and axillary lymph node3 (0/0); total (2/3): PNE (-, Maximal diameter: 3mm) - ER, PR, HER-2, Ki-67 (90/90/0/6.5%) Lum A Oncotype Dx: RS 10 CTx omission
Ours	# 1. Breast, RLO 09:00 4cm FN RMC 03:00 3cm FN, IDC, Multifocal, pT1cN1aM0, stage IIA - Histologic type: Invasive ductal carcinoma, NOS - Tumor margin: Infiltrative - Maximum diameter of invasive tumor: 1.5cm and 0.4cm - Maximum diameter of invasive and in situ carcinoma: 3.0cm - Nuclear grade: 2 - Histologic grade: II (3-2-1) - Lymphovascular invasion: Absent - Perineural invasion: Absent - Intraductal carcinoma component - Proportion: 10% - Extensive intraductal component (EIC): Absent - Type: Cribriform - Nuclear grade: Low - Necrosis: Absent - Location: Periphery - Calcification: Present (Malignant abd benign) - Associated benign lesion: Intraductal papilloma, sclerosing adenosis and columnar cell lesion - Resection margins - Overlying skin (superficial margin): Free of carcinoma (safety margin: 1.4cm) - Underlying fascia (deep margin): Free of carcinoma (safety margin: 2.3cm) - Lymph nodes, total (2/13): PNE (-), max 3mm - Axillary (0/10): Free of carcinoma - Sentinel lymph node1 (1/1), axillary lymph node1 (1/1), axillary lymph nodes without perinodal soft tissue extension (Maximal diameter: 3mm) - ER/PR/HER2/Ki-67 (90/90/0/6.5%) Lum A
Chat- GPT	Oncotype DX RS: 20 Adj. CTx omission #1. Breast, RLO 08:00, 15mm, IDC, pT1cN1(f)M0, Stage IIA ypT2 0cN0M0 - two (1.5cm and 0.4cm), H2N2 - two of 13 + - IVI (-), DLI (-), HD (-) - Extensive IC: (-) - Calcification (+) - RM (-) - Overlying skin: Free of ca (safety margin: 1.4cm) - Underlying fascia: Free of ca (safety margin: 2.3cm) - ER/PR/HER2/Ki-67 90/90/0/6.5% Lum A

Table S5: Example case for the plan suggestion task compared to baseline methods. The **red** scripts indicate the incorrect answers.

Example 1		
User	Suggest a radiotherapy approach using the guidance from the given clinical summary of the radiation oncologist. $\#$ Input: [Clinical notes]	
Ground truth	RT to WB and tumor cavity (SIB) 40.05 Gy $/$ 48 Gy in 15 fx.	
Ours	RT to whole breast $+$ tumor cavity (SIB) 40.05 Gy $/$ 48 Gy in 15 fx.	
Med-Alpaca	Breast, RUC, 12:00, 5cm FN, IDC, pT1cN0M0, stage IA	
ChatDoctor	\dots Depending on the patient's individual circumstances, the radiation oncologist may recommend course of external beam radiation therapy, brachytherapy, or a combination of the two \dots	
Chat-GPT	RT to right breast Conventional fractionation Total dose: 50 Gy in 25 fractions.	
Example 2		
User	Plan a radiotherapy treatment based on the insights from the radiation oncologist's clinical note. #Input: [Clinical notes]	
Ground truth	RT to Rt. chest wall + AXL Lv 3, IMN, SCL 40.05 Gy / 15 fx.	
Ours	RT to Rt. chest wall, AXL Lv 3, IMN, SCL 40.05 Gy $/$ 15 fx.	
Med-Alpaca	Status post core biopsy of the right breast, performed \dots	
ChatDoctor	\dots Deliver a dose of 40 Gy in 10 fractions over 4 weeks to the primary tumor, with a margin of 1.1 cm for the overlying skin and 1.2 cm for the underlying fascia. \dots	
Chat-GPT	RT to chest wall, IMN, and AXL Conventional fractionation 40.05 Gy / 15 fx.	
Example 3		
User	Considering the clinical insights from the radiation oncologist's note, set a treatment plan in terms of radiotherapy. # Input: [Clinical notes]	
Ground truth	RT to Lt. WB and tumor cavity (SIB) 40.05 Gy / 48 Gy in 15 fx (2.67 Gy / 3.2 Gy in daily fx).	
Ours	RT to Lt. WB and tumor cavity (SIB) $40.05~\mathrm{Gy}$ / $48~\mathrm{Gy}$ in $15~\mathrm{fx}$ (2.67 Gy / $3.2~\mathrm{Gy}$ daily fx)	
Med-Alpaca	Lymph nodes, total (0/4): Free of carcinoma - Sentinel lymph node1 (0/1), sentinel lymph node2 (0/1), sentinel lymph node3 (0/1), and axillary lymph node1 (0/1); total (0/4): Free of carcinoma	
ChatDoctor	\dots Radiotherapy will be administered to the breast, left, 2 o'clock, 4 cm FN IDC, pT1bN0M0, H1N2, PNI (-), LVI (-), EIC (-), Calcification: \dots	
Chat-GPT	RT to Left breast Conventional fractionation $40.05~\mathrm{Gy}$ / $15~\mathrm{fx}$.	
Example 4		
User	Considering the clinical insights from the radiation oncologist's note, set a treatment plan in terms of radiotherapy. $\#$ Input: [Clinical notes]	
Ground truth	RT to Lt. WB/Cavity, AXL 2, 3, Lv 4 (ESTRO), IMN 40.05 Gy $/$ 48 Gy in 15 fx (2.67 Gy $/$ 3.2 Gy in daily fx).	
Ours	RT to Lt. WB/Cavity, AXL 2, 3, Lv 4 (ESTRO), IMN 40.05 Gy / 48 Gy in 15 fx (2.67 Gy / 3.2 Gy daily fx).	
Med-Alpaca	ER: 20% of the tumor cells express nuclear signals of moderate intensity PR: Negative \dots	
ChatDoctor	\dots These findings suggest that the patient has an aggressive form of breast cancer and may benefit from additional chemotherapy and targeted therapy. \dots	
Chat-GPT	RT to left chest wall and axilla Conventional fractionation 40.05 Gy $/$ 15 fx for chest wall 40.05 Gy $/$ 15 fx for axilla.	

I Examples of Entire Workflow

We present examples of the entire workflow as indicated in Table S6 and Table S7. RO-LMM can take input as a pair of MRI report and Pathology report or another

pair of Ultrasound report and Pathology report. Our model seamlessly serves as an assistant for radiation oncologists by conducting report summarization, treatment plan suggestion, and 3D Target Volume Segmentation.

Table S6: Example of Entire Workflow in the case of taking MRI report and Pathology report as input.

User	Using the provided MRI and pathology findings, design a radiation oncologist's clinical overview $\#\#$ Input: [MRI report] [Pathology report]
RO-LMM-S+	#1. Breast, ROC, 09:00, 3cm FN, IDC, icT2N1(f)M0 stage IIB (anatomic), stage IIIB (prognostic) ypT0N0M0 [ic] T: - 39mm size mass, H3N3 - LVI (-) N: - Multiple suspicious lymph nodes at Rt. axilla level 1, 2, 3 (FNA+) *ER/PR/HER2/Ki-67 (-/-/3+/31.48%) HER2 positive (non Lum) [yp] - No residual ca - Fibrosis with hemosiderin laden macrophages and foam cell collection, favoring regressed tumo bed - Total LNs (0/25): Axillary (0/11), Level II (0/6): SLN (0/4), axillary (non SLN) (0/4) - Calcification (+, Benign) - RM (-): Nipple, upper, and lower margin: Free of carcinoma (See SF21-04688) * Lymphedema prediction - 2yr risk: 17.70% - 3yr risk: 20.28% - 5yr risk: 20.28% - 5yr risk: 22.97%
User	Suggest a radiotherapy approach using the guidance from the given clinical summary of the radiation oncologist. ## Input: [Generated Clinical Note]
RO-LMM-P++	$\overline{ m RT}$ to Rt. whole breast + AXL Lv 3 + SCL 48 (SIB) - 40.05 Gy $/$ 15 fx.
User	Draw the radiotherapy target volume of this patient with following planning CT scan. ## Input:[Generated Treatment Plan] [3D CT Scan] patient001.dcm
RO-LMM-SEG++	patient001_segmentation.dcm

Table S7: Example of Entire Workflow in the case of taking Ultrasound report and Pathology report as input.

User	Summarize a clinical summary note as a radiation oncologist might, using the provided Ultrasound and pathology details. ## Input: [Ultrasound reports] [Pathology reports]
RO-LMM-S+	#1. Breast, LUO 02:00 2cm FN, IDC, pT1cN0M0, stage IA - Histologic type: Invasive ductal carcinoma - Tumor margin: Infiltrative - Nuclear grade: 2 - Histologic grade: II (3-2-1) - Maximum diameter of invasive tumor: 1.4cm - Maximum diameter of invasive and in situ carcinoma: 2cm - Lymphovascular invasion: Not identified - Perineural invasion: Not identified - Intraductal carcinoma component: Present - Proportion: 35% (Extensive) - Type: Solid / Cribriform - Nuclear grade: Intermediate - Necrosis: Present (Comedo) - Location: Central and periphery - Calcification: Present (Malignant and benign) - Tumor infiltrating lymphocytes, stromal: < 10% - Resection margin: - Upper, lower, inner and outer margin: Free of ca - Total LNs (0/11): SLN (0/6), non SLN (0/5) ER: Positive (AS 8 = PS 5 + IS 3) PR: Positive (AS 5 = PS 3 + IS 2) HER2: Negative (1+) AR: Positive (AS 7 = PS 5 + IS 2) Ki67 L.I.: 20.8%in tumor cells - ER/PR/HER2/Ki-67 100/100/1+/20.8% Lum B (HER2 negative)
User	Suggest a radiotherapy approach using the guidance from the given clinical summary of the radiation oncologist. ## Input:[Generated Clinical Note]
RO-LMM-P++	RT to Lt. whole breast 26 Gy $/$ 5 fx $+$ 10 Gy $/$ 5 fx boost.
User	Draw the radiotherapy target volume of this patient with following planning CT scan. ## Input: [Generated Treatment Plan] [3D CT Scan] patient002.dcm
RO-LMM-SEG++	patient002_segmentation.dcm

J Prompt for Evaluation of Treatment Plan Suggestion

In this paper, we design prompts for evaluating generated treatment plans, including a reference-guided score rubric curated by clinical expert, as shown in Table S9. Similar to previous GPT-based evaluation methods, we tailor the prompts combining the specific knowledge of clinical experts. By using this prompt, we evaluate the results of our RO-LMM and all the baseline methods using GPT-4.0.

Table S8: Used prompts with proposed expertise-based rubrics for assessing the performance of treatment plan suggestion.

 $Based \ on < Ground \ Truth \ Plan>, \ score \ 1 \ if < Model \ Generated \ Plan> \ satisfies \ each \ rubric, \ else \ score \ 0.$

[Rubric]

R1. Laterality. Whether orientation (Rt./Lt.) is correct

R2. Aim of Surgery. Whether aim of RT (definitive RT = RT after breast conservation surgery or partial mastec-

tomy. In this scenario, breast should be irradiated. / postop RT = RT after total or radical

mastectomy. In this scenario, chest wall should be irradiated) is correct.

R3. Treatment Scope. Whether detailed extent of radiation field (inclusion or exclusion of WB, CW, AXL, SCL, \overline{MN}) and detailed level of inclusion (RTOG = in this guideline, upper SCL node is included

/ $\operatorname{ESTRO} = \operatorname{in}$ this guideline, upper SCL is not included) is correct.

R4. Dose Scheme. Whether RT scheme (dose in Gy, and fractions in fx) is correct. It also included SIB or

sequential boost dose.

R5. Hallucination. Whether unnecessary information is added or not (If unnecessary & incorrect information

was added, score 0 points, otherwise score 1 point)

[Abbreviations]

Radiotherapy RT.

BCS. Breast Conserving Surgery

PMRT. Post Mastectomy Radiation Therapy IMRT Intensity Modulated Radiation Therapy

PBI. Partial Breast Irradiation

SIB Simultaneous Integrated Boost technique, same as tumor bed boost (sequential), fast-forward

protocol

SCL. Supraclavicular Lymph Node IMN. Internal Mammary Lymph node

AXL. Axilla Lymph Node RTOG.

Radiation Therapy Oncology Group ESTRO. European Socity for Radiotherapy and Oncology

CW. Chest Wall Whole Breast WB.

[Ground Truth Answer Begin] < Ground Truth Plan> [Ground Truth Answer End]

[Model Responses Begin] <Model Generated Plan> [Model Responses End]

[Answer Format]

Model, Answer for R1, Answer for R2, Answer for R3, Answer for R4, Answer for R5, (scores ONLY for each Rubric in a tabular format, without explanation):

 $\textbf{Table S9:} \ \ \textbf{The proposed expertise-based rubrics for assessing the performance of clinical report summarization.}$

Based on rubrics, score each clinical report summarization.		
[Rubric]		
Rubric 1: Relevance	Assessment of whether the necessary information from the Ground Truth (GT) is included, and identification of any extraneous information	
	Good (2): The information from the GT is appropriately included.	
	Partially correct (1): Some relevant information is included, but there are omissions or irrelevant details.	
	Mostly irrelevant (0): The majority of the information is unnecessary or irrelevant.	
Rubric 2: Formatting	Evaluation of whether the necessary information is presented in the correct format and location:	
	Incorrectly placed (0): Information is not presented in the appropriate format or location.	
	Correctly placed (1): The necessary information is accurately positioned in the expected format.	
Rubric 3: Length	Assessment of whether the writing is excessively verbose:	
<u> </u>	Too verbose (0): The writing is overly lengthy and lacks conciseness.	
	Sufficiently summarized (1): The content is effectively summarized without unnecessary verbosity.	
Rubric 4: Consistency	Identification of conflicting information between sources:	
	Present (0): Conflicting pieces of information are observed.	
	Absent (1): There are no conflicting pieces of information between sources.	